

Supporting Information: Quantitative Magnetic Separation of Particles and Cells using Gradient Magnetic Ratcheting.

Authors: Coleman Murray, Edward Pao, Peter Tseng, Shayan Aftab, Rajan Kulkarni, Matthew Rettig, and Dino Di Carlo

Table of Contents:

Figure S1	p. 2
Figure S2	p. 3
Figure S3	p. 4
Figure S4	p. 5
Figure S5	p. 6
Figure S6	p. 7
Figure S7	p. 7
Figure S8	p. 8
Figure S9	p. 9
Figure S10	p. 10
Supporting Information – numerical simulations	p. 11
Figure S11	p. 11
Supporting Information – materials and methods	p. 12
Supporting Video Captions	p. 14

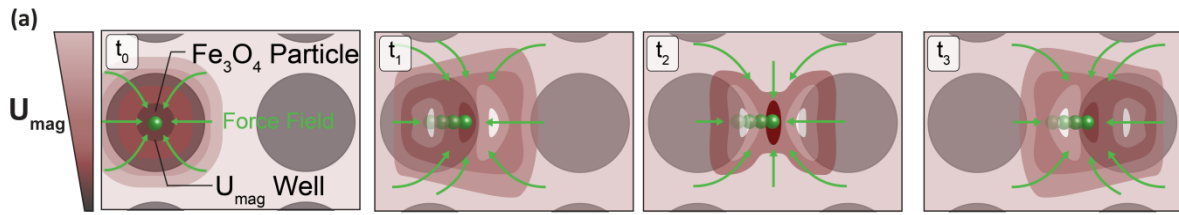


Figure S1: Magnetic ratcheting utilizes arrays of electroplated permalloy micro-pillars to modify the magnetic potential energy landscape (U_{mag}), creating dynamic potential energy wells to trap and manipulate superparamagnetic particles. When a bulk magnetic field is applied, the micro-pillars magnetize in alignment to the bulk field and modify the magnetic potential energy landscape introducing dynamic potential wells in which superparamagnetic particles become trapped. As the field orientation is cycled particles will follow the changing potential wells and ratchet through the pillars if the frequency and pitch between neighboring pillars is low enough and iron oxide content is high enough.

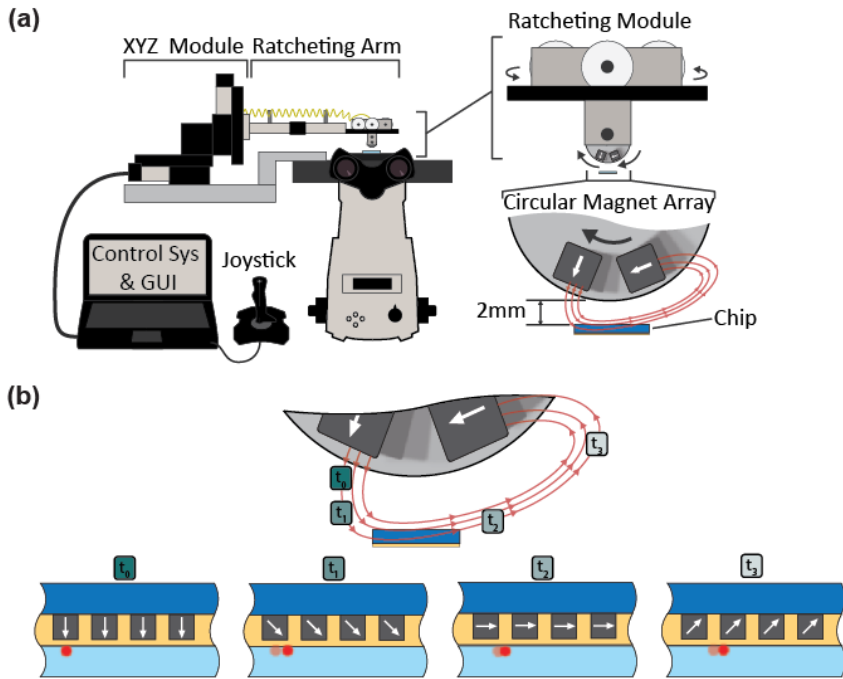


Figure S2: Automated and scope mounted ratcheting system consists of an XYZ module for positioning and a ratcheting module for angular and ratcheting speed control (a). The chip is first inverted onto a PDMS well containing aqueous buffer, placed on the scope, and then the ratcheting system is positioned over it with an offset of 2mm (a & b). The system was able to operate a full cycle of the radial array at frequencies between 0.1 to 50 Hz. Note that the mechatronic system was aligned to the ratcheting chips such that the central axis of the ratcheting module was aligned with the centroid of the ratcheting chip. The centroid for both chip designs was approximately 14mm from the chip's left edge and 0.5cm from the top edge. Alignment was performed as precisely as possible with a tolerance of approximately ± 5 mm. However, device performance is not highly sensitive to chip/mechatronic system alignment due to the fact that mm scale differences over the macroscale magnetic field de-amplify to nanometer scale changes of the micro-magnetic field within the permalloy micropillars.

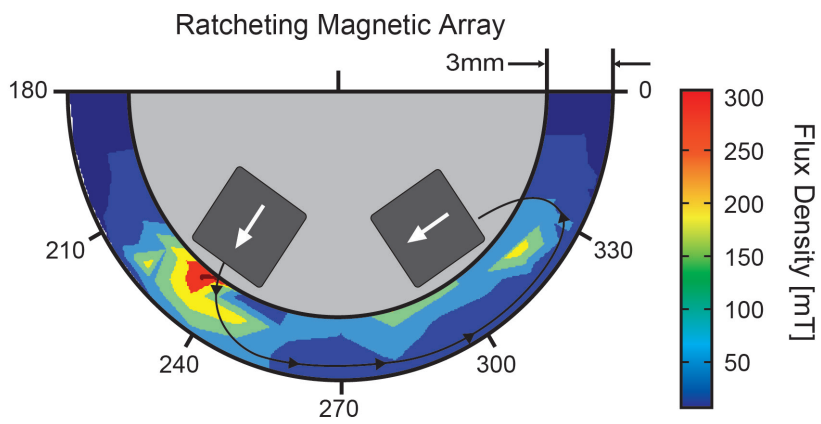


Figure S3: Magnetic wheel with a partial halbach array of N-52 grade rare earth magnets. As shown the peak flux density is 300mT with an average flux density of ~ 100 mT with a max radial distance of 3mm from the surface of the drum.

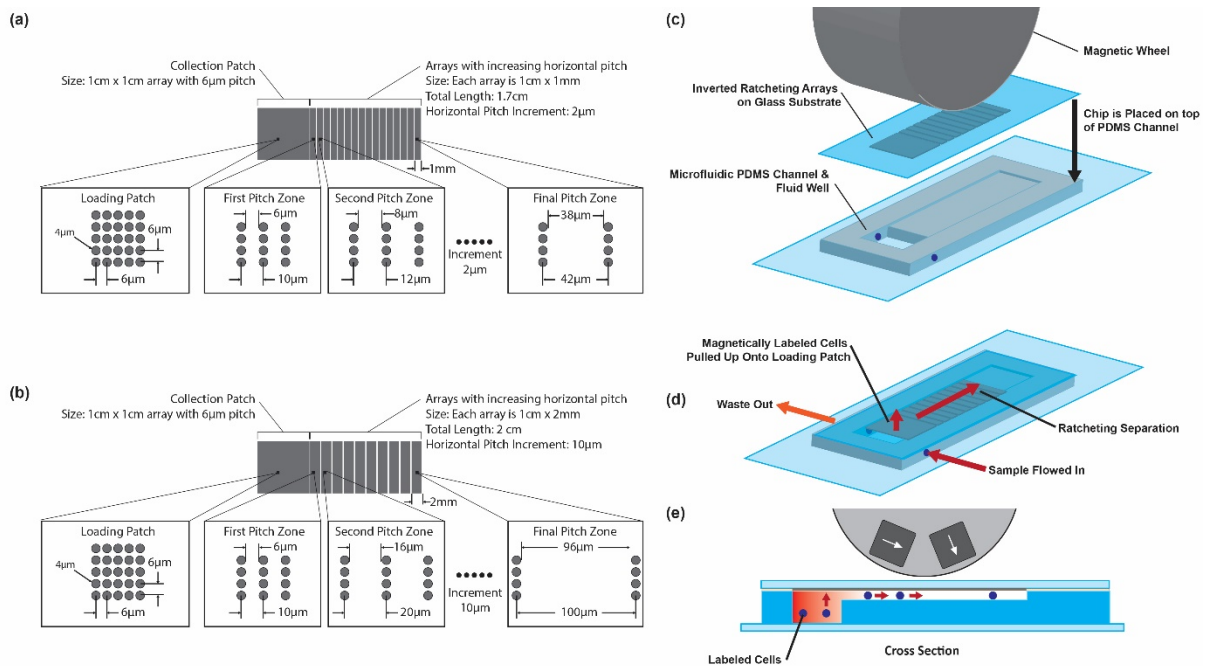


Figure S4: Schematic of gradient pitch arrays for ratcheting separation. Both chips consist of a 1 cm x 1 cm loading patch with 6 μm horizontal and vertical pillar pitch where samples containing cells were loaded or flowed over. Going from left to right, the loading patch leads into pitch zones of incrementally increasing horizontal pitch but a constant 6 μm vertical pitch throughout. (a) The first chip consists of seventeen, 1 mm x 1 cm pitch zones, where the first pitch zone has a 10 μm pitch (6 μm edge to edge gap) and increments by 2 μm with each zone; ending in a 42 μm pitch. (b) The second chip consists of ten, 2 mm x 1 cm pitch zones, where the first pitch zone has a 10 μm pitch, increments by 10 μm, and ends in a 100 μm pitch. (c) To achieve separation chips were inverted and placed onto an open air microfluidic PDMS chamber/channel produced using scotch tape lithography which was prefilled with PBS. The magnetic wheel from the mechatronic system was positioned directly above the inverted chip. (d-e) Sample was injected into the PDMS channel and the magnetically labeled cells were pulled up via the magnetic wheel and accumulated on the ratcheting array loading patch where they were separated after the entire sample volume was injected.

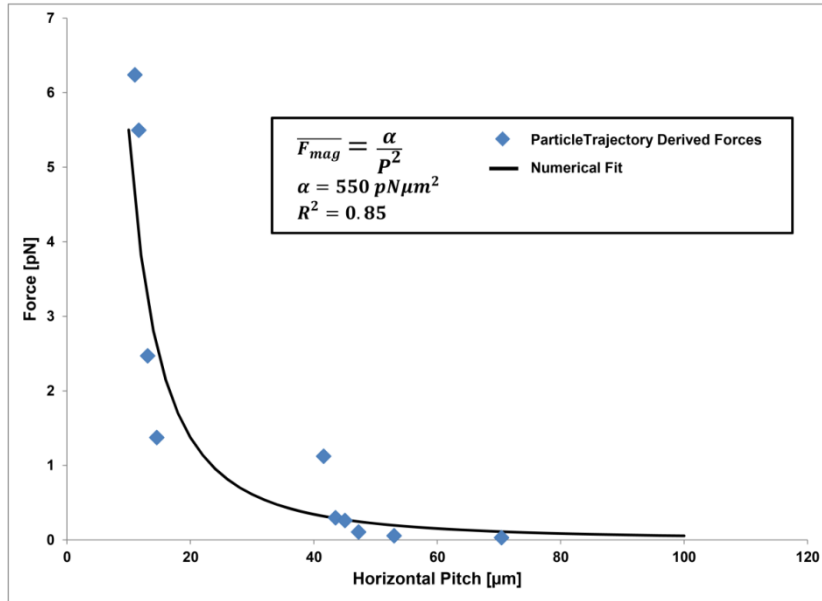


Figure S5: Calculated magnetic force on a $1\mu\text{m}$ particle vs. horizontal pitch which was determined empirically by tracking ratcheting trajectories of $1\mu\text{m}$ Fe_3O_4 particles at various frequencies on $10\mu\text{m}$ incremented chip by balancing with drag force. A power law best fit the data, specifically αP^{-2} , where $\alpha=550\text{pN}\mu\text{m}^2$. Pearson's fit coefficient for this data was 0.85.

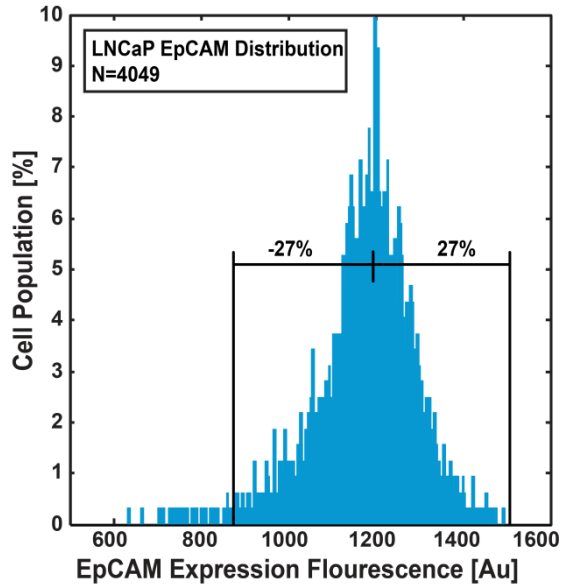


Figure S6: Flow cytometry analysis for EpsCAM expression on LNCaP cells. The EpCAM expression shows a near normal distribution with approximately a 27% coefficient of variation.

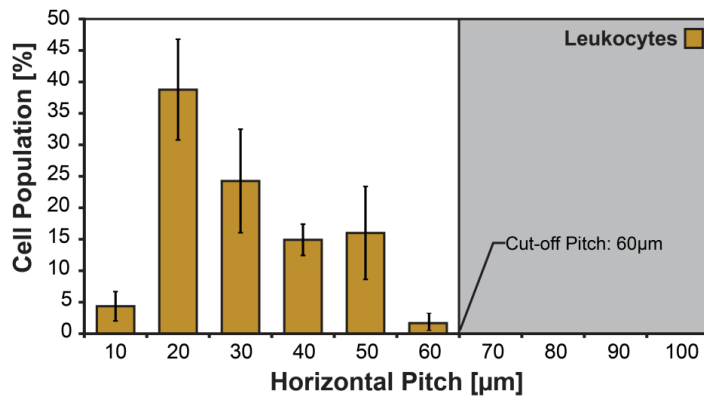


Figure S7: Healthy control samples (N=3), including 1 age matched sample, was run through the chip to develop a healthy patient profile and determine cutoff pitch for leukocyte background. The non-specifically labeled leukocyte population occupied the 10-60 μ m pitches under a 5Hz ratchet, therefore the cut-off pitch was set as $\leq 60\mu$ m and cells equilibrating at $\geq 70\mu$ m under a 5Hz ratchet were past the leukocyte background.

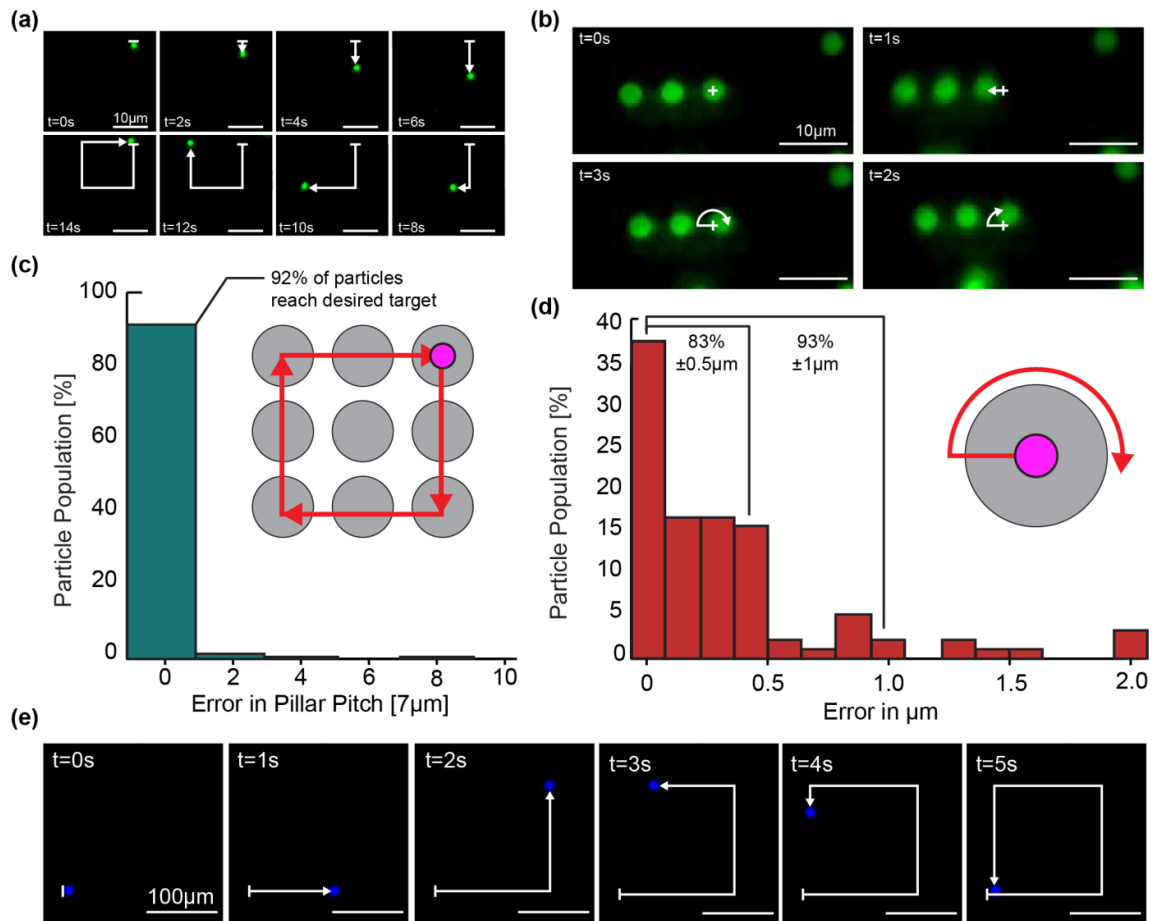


Figure S8: Using the automated ratcheting system parallelized and high resolution manipulation of particles and cells can be achieved. (a) Coarse mode manipulations of $2.8\mu m$ particles in a square trajectory can be achieved by translating particles between pillars and (b) fine mode, nanometer scale manipulations can be achieved by piloting the particle radially and tangentially on a single pillar. (c) Coarse mode manipulations have high consistency where 92% of particles were successfully piloted to a desired location. (d) Fine mode manipulations demonstrated nanometer scale error with 83% of the particles having a ± 500 nm error and 93% of the particle population had a $\pm 1\mu m$ error. (d) Cells can also be piloted in an arbitrary trajectory in a parallelized and repeatable manner.

Particle Distributions within 10 μ m Incremented Chip

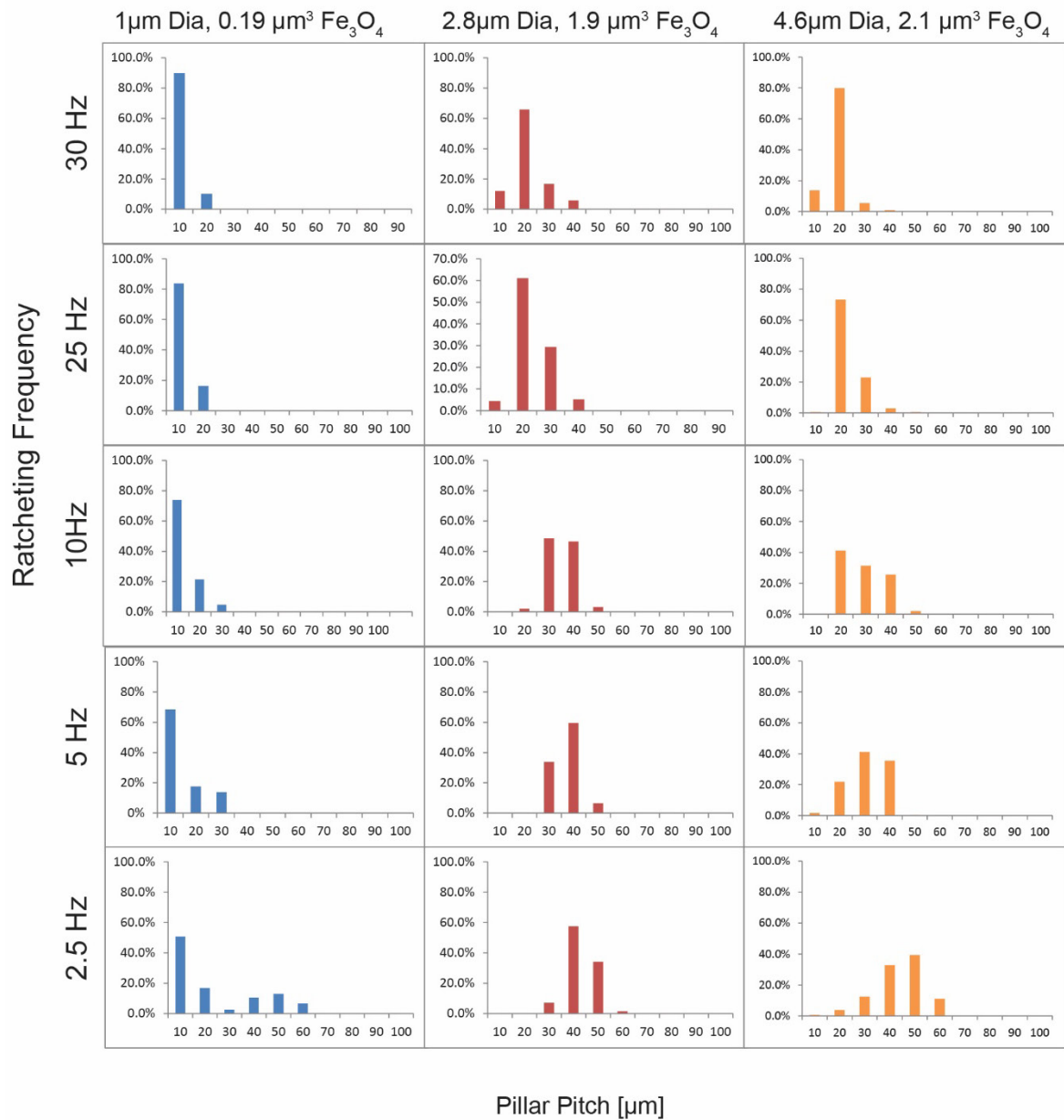


Figure S9: Shown above are distributions of several particle types (1 μ m, 2.8 μ m and 4.6 μ m diameter) driven at 30, 25, 10, 5 and 2.5 Hz ratcheting. As expected, particles with higher iron oxide content equilibrate at larger pillar pitches. As frequency decreases, the particle population migrates to higher pitches.

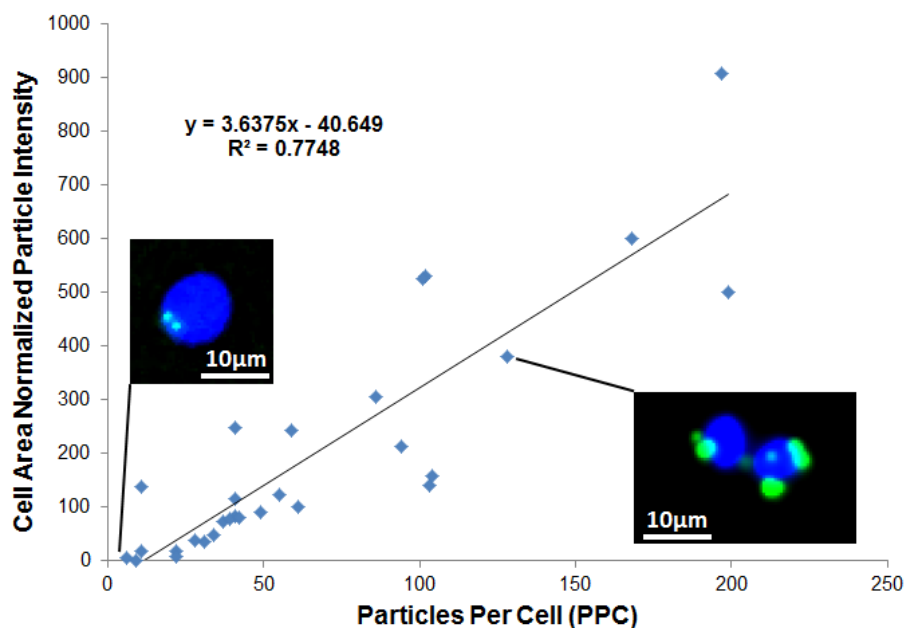


Figure S10: The quantity of bound particles on magnetically labeled cells was determined using florescent image analysis. The intensity values from the bound particles (green) was summed over each cell and divided by the nuclear area (blue) to provide a cell area normalized particle intensity value. A calibration curve between the cell area normalized particle intensity value and particles per cell (counted manually in Image J) was generated to quantify the number of bound particles. This calibration curve was used to determine PPC values for separation on gradient pitch arrays.

Supporting Information: Numerical Simulations

Permalloy Micro-pillar Aspect Ratio vs. Force Application

One of the peak challenges for translating magnetic ratcheting into biomedical application is attributed to the minimal force envelope. Traditional ratcheting platforms consist of thin magnetic structures (aspect ratios ~ 0.05) which are usually fabricated using metal evaporation. However, thin film structures are limited in the forces they can apply due to minimal amount of volume in the ratcheting elements. As shown in **Figure S11a-b**, numerical simulations of the micro-magnetic field with various pillar aspect ratios were performed using the Magnetostatics Module Comsol 4.2. As shown in **Figure S11c**, the peak magnetic force decreases rapidly with aspect ratio.

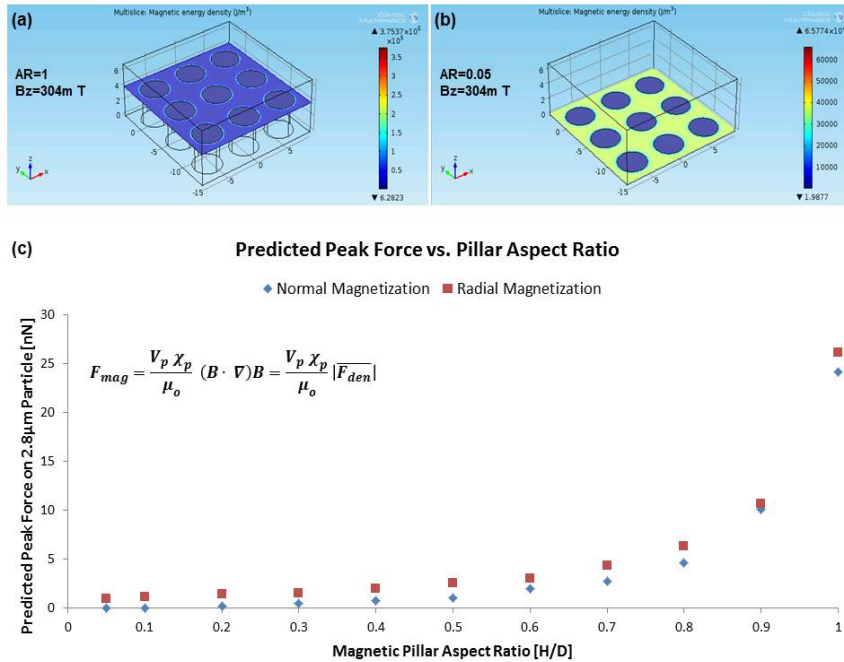


Figure S11: Predicted peak force on a 2.8μm magnetic particle ($V_p=1.95\mu\text{m}^3$, 17% Fe_3O_4 , $\chi=0.65$, $\mu_0=4\pi \cdot 10^{-7}$) as a function of pillar aspect ratio was simulated using Comsol 4.2 Magnetostatics Module. In the simulation the pillars were set to have a relative magnetic permeability of 8500, a diameter of 4μm, an orthogonal pitch of 6μm and a height derived from the corresponding aspect ratio (a & b). Boundary conditions included a 304mT inward flux density with either a normal orientation (parallel to the pillar axis) or tangential (parallel to the pillar radii). The force density, defined as $(B \cdot \nabla)B$, was numerically calculated at the surface of each pillar and the magnetic force derived for a 2.8μm magnetic particle (c).

The limitation on the force envelope has limited thin film ratcheting to use larger magnetic particles (2.8μm and above) to compensate. However, larger particles are less ideal for magnetic labeling applications due to their limited diffusivity which results in low labeling efficiency. The presented system overcomes these challenges, with aspect ratios ~ 1 , thereby allowing the use of smaller particles (1μm and under) and enabling magnetic ratcheting to be used as a quantitative separation technology.

Supporting Information: Materials and Methods

Chip Fabrication

Polished borosilicate glass (Fisher) were cleaned with piranha solution (30 min), washed in DI water and dried before deposition of 50-nm-Ti, 200-nm-Cu and 50-nm-Ti seed layer using a CHA Mark 30 E Beam Evaporator. SPR 220 photoresist was spun and processed according to specification to form electroplating molds for nickel-iron alloy. Ti was etched in 1% HF, and NiFe was electroplated in a custom plating setup to a $\sim 4\mu\text{m}$ thickness. Photoresist was stripped and both the Ti and Cu layers were etched completely. The chip was sealed by deposition of 100 nm SiN (PECVD). Spin on polystyrene was spun to a thickness off $\sim 1\mu\text{m}$ above the pillars. Before use, substrates were immersed in 2% by volume Pluronic F127 for 45 minutes.

Particles and Particle Separations

Streptavidin coated $1\mu\text{m}$ and $2.8\mu\text{m}$ IO particles, 37% and 17% IO content respectively (Invitrogen), were functionalized with biotinylated fluorescent probes (Invitrogen). $4.6\mu\text{m}$ biotinylated particles (Spherotech 4.5% IO) coated with streptavidin then with fluorescent biotin. $5\mu\text{m}$ polystyrene magnetic particles (Sigma, 20% IO) were aminated via perfluoroazide and made fluorescent with Alexa Fluor hydrazide (Invitrogen). Particles were diluted to working concentrations between $0.5\sim 1 \times 10^6$ **particles/mL**. PDMS interface chips (Dow-Corning) were fabricated using scotch tape lithography and clamped to the ratcheting chips using a custom made polycarbonate clamp. Separation experiments were executed by inverting the chip on the stage of a Nikon Eclipse Ti fluorescent microscope and positioning the ratcheting system above it. Particles were injected into the ratcheting chip, ratcheted at various frequencies, and imaged under 10X objective using the DAPI, FITC and TRITC filter sets. Image analysis using ImageJ was used to identify equilibrium particle distributions on the chip for varying frequencies.

Image Analysis to Determine Quantity of Particles Per Cell (PPC)

The quantity of bound particles per cell was determined using image analysis of fluorescently labeled cells and particles. After cells were magnetically labeled with $1\mu\text{m}$ iron oxide particles functionalized with mouse anti-EpCAM, the particles were fluorescently labeled with anti-mouse 488 antibody and the cell nuclei were labeled with Hoesch. Therefore, both cells and particles could be visualized and imaged fluorescently for analysis. As a metric, the intensity values from the bound particles was summed over each cell and divided by the nuclear area to provide a cell area normalized particle intensity value. A calibration curve between the cell area normalized particle intensity value and particles per cell (counted manually in Image J) was generated to quantify the number of bound particles (Figure. S 10). Cells separated on the gradient pitch chips were imaged under a fluorescent microscope and each cell was cropped into an individual frame for analysis. Using a Matlab® script, the cell area normalized particle intensity value was determined, and the PPC value was determined using the calibration curve.

Blood Spiking, Capture Efficiency and Purity Experiments

Peripheral whole blood was collected from healthy donors, including 1 age matched donor, and aliquoted into 1mL volumes. ~ 100 LNCaP cells were pre-labeled with Celltracker Green (Invitrogen) and spiked into the blood. The blood was then diluted 5x with pbs and $1\mu\text{m}$ anti-EpCAM particles were added to a final concentration of 10^6 particles/mL. The samples were incubated at room temperature for 2 hours with gentle agitation and stained with Hoescht to

visualize cell nuclei. The total volume was injected through the magnetized chip at 50 μ L/min. Ratcheting separation was carried out at 5Hz and the entirety of the chip was imaged under DAPI and FITC wavelengths. Capture efficiency was determined by counting the number of FITC positive cells and comparing to a control. Purity characterization was performed similarly where ~2000 FITC labeled LNCaP cells were spiked into 1mL of whole blood, labeled, then separated at 5Hz. Purity was defined as the ratio of spiked LNCaP cells to the total number of cells binned by pitch.

Ratcheting Cytometry with Prostate Cancer Patients

Blood from patients with metastatic castration resistant prostate cancer was aliquoted into 1mL volumes in Falcon tubes. 12 μ L of anti-CD45 PE was added to label all white blood cells and 2 μ L of Hoechst stain was added to label all nuclei and allowed to incubate for at 30 minutes. The sample was then diluted to 5X with PBS, 1 μ m anti-EpCAM particles were added to the blood at 10⁶ particles/mL, and allowed to incubate for 2 hrs under gentle agitation. The solution was then injected over the magnetized chip loading patch using a syringe pump set to 50 μ L/min. Once injected through the chip, the cells were separated using a 5Hz ratchet and the chip was imaged at 10x magnification under DAPI and TRITC wavelengths.

Supporting Video Captions

Movie S1:

Mechatronic ratcheting system can be mounted onto an inverted microscope for ratcheting of magnetic particles and cells across permalloy micro-pillar arrays. The system generates a cycling magnetic field using a wheel of rare earth magnets arranged in a halbach array orientation. The system can also be controlled to adjust the in plane ratcheting angle for separation and concentration functions. Ratcheting control can be achieved via a joystick or by an automation program for hands free manipulation and separations.

Movie S2:

Green fluorescent 2.8 μm superparamagnetic particles ratcheted on a permalloy micro-pillar array chip with gradient horizontal pitch. If the pitch is less than equal to the critical pitch, the particle will traverse the array. If the pitch exceeds the critical pitch, the particles will trap and coalesce. Critical pitch is dependent on the particle's iron oxide content.

Movie S3:

LNCaP cells magnetically labeled with αEpCAM 1 μm diameter superparamagnetic particles can be quantitatively separated based on the quantity of bound particles. Cells will traverse the array until reaching their critical pitch where they will equilibrate and concentrate.

Movie S4:

After quantitative separation, cells can be further concentrated for extraction off chip. By ratcheting orthogonally to the chip, cells can be transported to the base of the chip and collected.

Movie S5:

Using the automated ratcheting system parallelized and high resolution manipulation of particles and cells can be achieved. Coarse mode manipulations of 2.8 μm particles in a square trajectory can be achieved by translating particles between pillars and fine mode, nanometer scale manipulations can be achieved by piloting the particle radially and tangentially on a single pillar. In addition to particles, cells can also be piloted in an arbitrary trajectory in a parallelized and repeatable manner. Shown are cell piloted in a square trajectory and a square wave trajectory.